

An error-mitigated photonic quantum circuit Born machine

Alexia Salavrakos,^{1,*} Tigran Sedrakyan,¹ James Mills,^{1,2} and Rawad Mezher¹

¹*Quandela, 7 Rue Léonard de Vinci, 91300 Massy, France*

²*School of Informatics, University of Edinburgh,
10 Crichton Street, Edinburgh EH8 9AB, Scotland*

Generative machine learning models aim to learn the underlying distribution of the data in order to generate new samples. Quantum circuit Born machines (QCBMs) are a popular choice of quantum generative models, which are particularly well suited to near-term devices since they can be implemented on shallow circuits. Within the framework of photonic quantum computing, we design and simulate a QCBM that can be implemented with linear optics. We show that a newly developed error mitigation technique called recycling mitigation greatly improves the training of QCBMs in realistic scenarios with photon loss.

INTRODUCTION

Generative learning has captured much attention in the field of classical machine learning over the last decade, with the advent of deep generative models like variational autoencoders (VAEs) [1], generative adversarial networks (GANs) [2], diffusion models [3], and most recently large autoregressive models [4]. Over the same period of time, the field of quantum machine learning has emerged and grown fast, with a recent focus on variational quantum algorithms [5], which are hybrid quantum-classical models that can be implemented on noisy-intermediate scale quantum (NISQ) devices [6]. In these algorithms, the model is implemented by a parametrized quantum circuit often called *ansatz*, and the parameters are optimized through a classical procedure. While classification tasks have been studied extensively [7, 8], considerable progress has also been achieved on quantum generative models [9]. Quantum GANs and quantum VAEs were introduced in [10, 11] and [12] respectively, while energy based models such as quantum Boltzmann machines were studied in [13, 14].

Quantum Circuit Born Machines (QCBMs) were introduced as a circuit-based model [15, 16], where the circuit *ansatz* prepares a state and the Born rule is naturally implemented by the measurements at the end of the circuit. These models are implementable on NISQ hardware, and a first experimental realization was obtained in [15] on an ion trap quantum processor. Since then, further demonstrations of QCBMs and QCBM-like models were realized on ion traps [17, 18], as well as on superconducting platforms [19–21].

Each platform that is being considered for the development of a quantum computer has its strengths and weaknesses, whose importance may vary according to the task at hand. Fast sampling, for instance, could be particularly interesting for generative learning, and is a benefit of

photon-based devices. In terms of single-photon-based devices, Quandela recently introduced a quantum processor called *Ascella* [22], made of a single-photon source supplying a universal linear optical network on a reconfigurable chip. *Ascella* can handle up to 6 photons in 12 modes. Photonic platforms are also known for demonstrations of quantum advantage [23, 24] via Gaussian boson sampling [25].

While such devices are currently state-of-the-art, they have not yet entered a regime where error correction (QEC) can be applied at scale. In contrast to QEC protocols, which require a large overhead of qubits to be realised [26], quantum error mitigation (QEM) replaces this qubit overhead with a sampling overhead. More precisely, QEM requires more runs of a quantum algorithm, but allows this algorithm to be run on a NISQ device without the need for any ancillary qubits [27, 28]. This makes QEM particularly useful for current and near-term quantum hardware. Photonic devices suffer significantly from a particular type of noise: erasure noise in the form of photon loss. In related work [29], a recycling mitigation technique is presented that deals with photon loss. This technique makes use of photonic output states that would normally be discarded in post-selection, and provably outperforms post-selection for up to large sample sizes.

In this work, after introducing a QCBM scheme for linear optical circuits, we show that its training is significantly improved by the recycling mitigation technique in realistic scenarios with photon loss. We demonstrate several situations where a QCBM becomes trainable if recycling mitigation is applied. In particular, we study in our simulations very high loss regimes and photon distinguishability, thus mimicking the conditions on current photonic quantum processors. In the discussion section, we consider the question of classical simulability and the link with boson sampling [30].

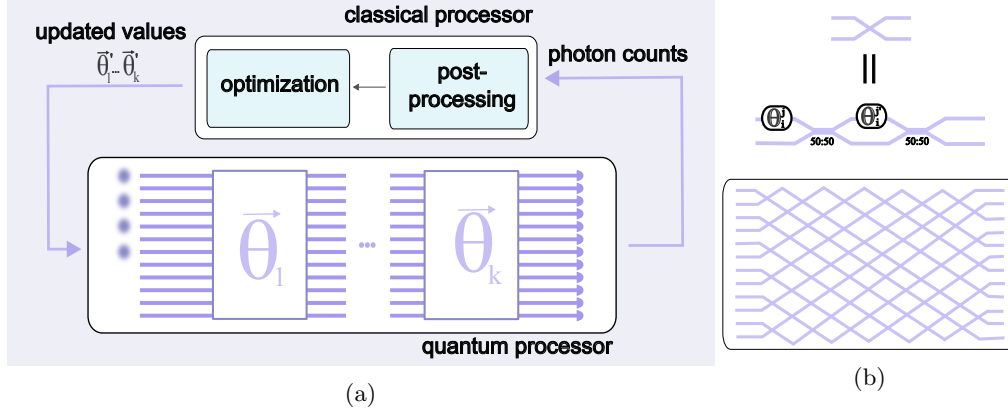


Figure 1: (a) QCBM ansatz pictured for a circuit with $m = 12$ modes and $n = 4$ photons and input Fock state $|101010100000\rangle$. We allow the variational blocks parametrized by $\bar{\theta}_i$ to be repeated k times. (b) One variational block is a universal interferometer. Each crossing between the optical modes $\bar{\theta}_i$ corresponds to a Mach-Zender interferometer that is parametrized by two phases.

A PHOTONIC QCBM

Generative learning. Given a set of data instances X and labels Y , while a discriminative or classification model aims at predicting $P(Y|X)$, a generative model seeks to estimate the joint distribution $P(X, Y)$, or simply $P(X)$ if there are no labels. If the model has parameters $\bar{\theta}$, a loss function \mathcal{L} is defined which should express how close the distribution of the generated samples is to the one of X . The loss is optimized so as to obtain $\bar{\theta}^* = \arg \min_{\bar{\theta}} \mathcal{L}(\bar{\theta}|X)$. Once the model is trained, it can be used to generate new samples with similar properties to the training dataset.

Photonic architecture. We propose using an ansatz based on the universal interferometer Clements scheme [31], as shown in Figure 1. We believe our choice to be well motivated, since the interferometer guarantees interactions between all modes, and allows for arbitrary unitary transformation on the modes to be realized. Additionally, it matches the scenario of boson sampling. Note that in [32] and [33], the authors present QCBMs with a different linear optical ansatz. The ansatz is the same in both articles and appears to mimic the gate-based ansatz of [16] by replacing two-qubit controlled gates with beam splitters and one-qubit gates with phase-shifters.

As can be seen in Figure 1, our QCBM ansatz consists of a linear optical circuit with m modes and n photons. It receives a Fock state as input: $|\vec{n}_{in}\rangle = |n_1^{in}, \dots, n_m^{in}\rangle$, where n_i^{in} indicates the number of photons in mode i and $\sum_i n_i^{in} = n$. This state is transformed according to the parametrized universal interferometer which implements a unitary $U(\bar{\theta})$. Indeed, the Clements

scheme allows for the decomposition of an arbitrary unitary into a product of $T(\theta_i^j, \theta_{i+1}^j)$ matrices. Each matrix corresponds to a Mach-Zender element between the j -th and $(j+1)$ -th modes, as depicted in Fig 1b, and has the form:

$$\begin{pmatrix} 1 & 0 & \dots & & \dots & 0 \\ 0 & 1 & & & & \vdots \\ \vdots & & e^{i\theta_i^j} \cos \frac{\theta_i^j}{2} & -\sin \frac{\theta_i^j}{2} & & \vdots \\ & & e^{i\theta_i^j} \sin \frac{\theta_i^j}{2} & \cos \frac{\theta_i^j}{2} & & \vdots \\ \vdots & & & & & 1 & 0 \\ 0 & \dots & & & \dots & 0 & 1 \end{pmatrix}$$

At the output of the circuit, the state is measured by photon detectors. The different Fock states $|\vec{n}_{out}\rangle = |n_1^{out}, \dots, n_m^{out}\rangle$ are detected as arrangements of photons in the output modes, that we denote $s = (n_1^{out}, \dots, n_m^{out})$. When photon loss is present, the n_i^{out} may not sum to n . Detecting all possible output states is not straightforward in practice because photon number resolving (PNR) detectors are not readily available with current technology. To match experimental settings, we make the simplifying choice of using threshold detectors in most of our simulations, thus only allowing n_i^{out} to be 0 or 1.

Then, outputs s are mapped through classical post-processing to the space of the data that the model aims to generate. For instance, if we consider simple one-dimensional numerical data X set between x_{\min} and x_{\max} , we proceed by binning the range of values $[x_{\min}, x_{\max}]$, then defining a mapping between each possible output and each bin. If the data is discrete, there is no need

for the binning, and a certain output s^* can directly be interpreted as a value x^* .

Training strategy. The model is trained as a variational algorithm, which means that a classical optimization procedure is applied to the model parameters θ , as shown in Figure 1. In most simulations, we use the Kullback-Leibler (KL) divergence [34] as a loss function. We recall the definition of the KL divergence, given two probability distributions Q and P defined on the same sample space \mathcal{X} :

$$D_{\text{KL}}(P||Q) = \sum_{x \in \mathcal{X}} P(x) \log \left(\frac{P(x)}{Q(x)} \right). \quad (1)$$

We also consider as metrics the Total Variational Distance (TVD) and the Maximum Mean Discrepancy (MMD) [35]. We refer the reader to the last section of this paper for a discussion around the choice of the loss function.

Gradient evaluation in quantum machine learning is less straightforward than in classical machine learning, due to the lack of an equivalent for the backpropagation algorithm. The parameter-shift method [36, 37] is the current standard for variational quantum circuits – however, to the best of our knowledge, only the recent work of [38] proposes parameter-shift rules adapted to photonic quantum circuits, and these require larger circuits for the gradient computation. Here, we use an optimizer based on the Simultaneous Perturbation Stochastic Approximation (SPSA) method [39]. This involves stochastic gradient approximation, thus allowing for fewer evaluations of the model at each step. We start the optimization by randomly initializing the circuit parameters $\vec{\theta}$.

RECYCLING MITIGATION

Recycling mitigation is a technique for mitigating the effects of uniform photon loss in linear optical quantum circuits consisting of single photons, multi-mode linear optical interferometers, and single photon detectors [29]. At the heart of recycling mitigation are the *recycled probabilities*, constructed from the statistics of the linear optical circuit affected by photon loss, that is, statistics where the number of detected photons at the output of the circuit is less than at the input. In quantum algorithms run on currently available photonic hardware [22], statistics where photon loss occurs are discarded, and only the statistics where no loss occurred are used for the computation. This procedure is referred to as post-selection, and is the standard method for

correcting the effects of photon loss in the above described linear optical circuits.

For a given output s of a linear optical circuit, as defined above, the recycled probability $p_R(s)$ is of the form

$$p_R(s) = p_1 p_{id}(s) + (1 - p_1) I(s), \quad (2)$$

where $0 \leq p_1 \leq 1$, $p_{id}(s)$ is the ideal probability of outcome s in the absence of photon loss, and $I(s)$ is the *interference term*, which is an artifact of constructing recycled probabilities from probabilities affected by photon loss. Applying certain classical post-processing techniques, detailed in [29], to the set of recycled probabilities $\{p_R(s)\}$ allows the recovery of a set of mitigated probabilities $\{p_{mit}(s)\}$, which are approximations of the ideal probabilities $\{p_{id}(s)\}$.

Recycled probabilities are constructed in such a way as to maximise the weight p_1 , corresponding to the *signal* of the ideal probability. Furthermore, expectation values of the interference term $\mathbb{E}_s(I(s))$ can be computed exactly, this allows the computation of concentration inequalities for $I(s)$. These facts, combined with the fact that the lossy probabilities used in constructing recycled probabilities have smaller statistical errors than post-selected probabilities, are central to why recycling mitigation outperforms post-selection up to large sample sizes.

The performance guarantees for recycling mitigation derived in [29] are for outputs s where at most one photon occupies a given mode. In the so-called no-collision regime where $m \gg n$ it is natural to expect such a behaviour of the outputs [30]. In our simulations however, m and n have a comparable size. We can map the simulated outputs s where more than one photon can occupy a mode to threshold outputs, and use them in the recycling mitigation, whereas in post-selection they are discarded and the distribution is renormalised.

NUMERICAL SIMULATIONS

Perceval [40] is a software platform for simulating discrete-variable photonic quantum computing. We use *Perceval* to simulate the QCBM scheme presented in the last section, for various scenarios. Given the same resources, we typically compare the following cases: the ideal lossless case, the lossy case described by loss parameter η , and the same lossy case where recycling mitigation was applied. Note that η expresses the probability that one photon is lost during the computation. Thus, when working with n photons, the

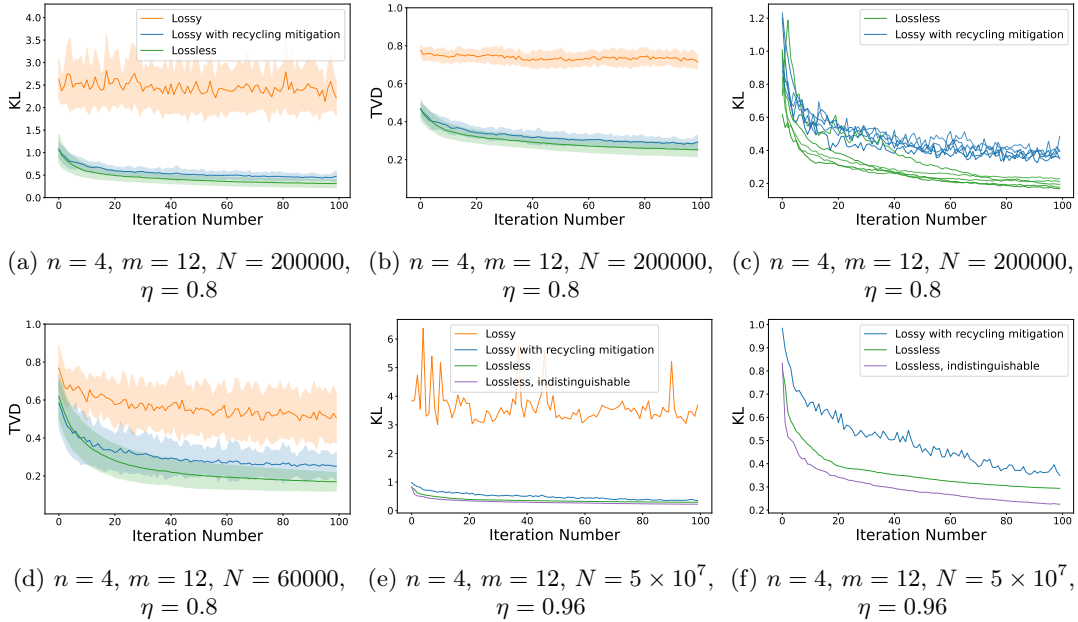


Figure 2: (a) Value of the KL loss function for the mixed Gaussian case, averaged over 20 training instances. The shaded area depicts a standard deviation from the mean. Each training instance has different initialization parameters. (b) Evolution of the TVD during those simulations. (c) We highlight the 5 best training instances out of the 20 simulations. (d) Value of the TVD loss function for the financial data for the EUR-USD currency pair, averaged over 20 training instances. (e) Training instance where the simulation is closely tailored to Quandela’s *Ascella* processor. All but one curve include photon distinguishability. (f) For this last training instance, we focus on both lossless cases and on the lossy case with recycling mitigation.

probability of observing n -photon counts at the output of the circuit scales as $(1 - \eta)^n$.

We denote by N the number of initial samples for a given simulation. Depending on the choice of loss function, these samples can either be input directly into the loss, or used to empirically estimate the output probabilities employed in the loss function. In the lossy case, for typical values of η , only a small fraction of N will be detected as n -photon counts. The n' -photon counts with $n' < n$ are discarded through post-selection, and the lossy QCBM is trained on this small post-selected fraction. Whereas, in the case where recycling mitigation is applied, information from the n' -photon counts is taken into account to train the QCBM, as explained in the previous section.

We summarise our results in Figure 2. As our main illustrative example, we consider in Figure 2a-2c the problem of learning a bimodal distribution consisting of two superimposed Gaussian distributions with different means, as in [41]. This distribution can be generated straightforwardly in Python. We observe that for given N and η , recycling mitigation significantly improves the training of lossy QCBMs, while the lossy unmit-

igated case remains untrainable. Recycling mitigation brings the value of the loss function close to the lossless one, as well as other metrics. We also note the importance of initialization parameters and the variance in the training process in Figure 2c.

As a second example, we consider financial foreign exchange data in Figure 2d and we use the TVD as a loss function, as we found it more suitable for a sparser distribution. We collect daily log returns of currency pairs over the last 20 years, as was done in [20]. This data simply describes the evolution of the exchange rate between pairs of currencies like EUR and USD. Instead of converting several currency pair values to binary strings, which was convenient for the qubit case and thus done in [20], we focus on one currency pair given one QCBM and we model it at a higher precision – which would correspond to using 7 qubits for one currency pair in that binary encoding.

During our training process, we compared different ansätze. We explored the case where $k > 1$ and the parameters are repeated between blocks $\vec{\theta}_1 = \vec{\theta}_2 = \dots = \vec{\theta}_k$, as well as the case where each Mach-Zender interferometer in a block is

parametrized by only one phase, the other one being set to 0, thus halving the total number of parameters. Overall, we observed the best results for a simple ansatz made of a single block ($k = 1$), keeping two parameters per interferometer. Most of our results are presented for loss parameter $\eta = 0.8$, which is within reach for near-term hardware [22].

Our results remain valid for higher values of η , as we show by closely modelling the conditions on Quandela’s *Ascella* quantum processor. The processor has 12 modes and corresponds exactly to our ansatz with $k = 1$. *Ascella* was estimated to have the following noise parameters at the time of our simulations: around 0.96 for photon loss, and around 0.08 for photon distinguishability. Note that this latter type of noise is also commonly encountered in photonic devices and would require a different kind of error mitigation. Due to the high loss regime, we use 5×10^7 samples at the input. As this slows down our simulations, we present our results in Figure 2e and 2f for one training instance only. As before, we observe a large gap between the unmitigated and mitigated lossy cases. We also note the effect of distinguishability, as the fully noiseless simulation reaches a lower value of the loss function.

In our simulations, we compared an error-mitigated QCBM with a lossy QCBM trained on the post-selected fraction of samples that correspond to n -photon counts. There could be two alternative strategies for dealing with losses: one would be to sufficiently increase the initial number of samples N so that the lossy unmitigated case becomes trainable. However, this strategy might require a lot of resources, especially in high loss regimes, where it would significantly increase the time required for a physical experiment. Another strategy would be to train the QCBM directly on lossy outputs, i.e. on n' -photon counts where $n' < n$, and map these outputs to the data that the model aims to generate. However, our tests indicate that such a strategy is not viable for the trainability of the model.

DISCUSSION

When considering quantum advantage of models based on linear optical circuits, it is natural to look for a connection with boson sampling. In this context, we note that generative models may be better candidates for a potential quantum advantage than classifiers obtained from a similar circuit, such as the ones in [22, 42]. Indeed, as Aaronson and Arkhipov pointed out in their original article [30], if the circuit is used for proba-

bility estimation instead of sampling, there is a polynomial-time (in the input size) classical algorithm by Gurvits which approximates the permanent of any submatrix of a unitary matrix to within polynomially-small additive error [43, 44]. This means that estimating the permanent from a polynomial (in input size) number of experiments does not yield an exponential advantage over classical algorithms estimating the permanent, by standard arguments from statistics [45].

Since photonic generative models like QCBMs are based on sampling rather than permanent estimation, the question of whether or not an exponential quantum advantage exists remains open. Although the precise relationship between photonic QCBMs and classical hardness would have to be clarified, as in [46], this reinforces the value of studying generative models within a native photonic framework.

While this observation holds true when using an already trained model to produce samples, it does not necessarily apply to the training phase of the model. For instance, in our training, we exploited the output probability distribution of the circuit, which allowed us to apply recycling mitigation. The use of an explicit loss function [47] based on the output probability distribution then comes at no additional cost, so it made sense for us to use the KL divergence or the TVD. On the other hand, the connection with classical hardness is less clear.

Nevertheless, this approach to training retains potential, as it turns out that there is still a small polynomial advantage in estimating probabilities given by the modulus squared of a permanent in a boson sampling experiment. Indeed, we show in the Appendix that statistics collected from t i.i.d runs of a boson sampler allow, with high probability, for estimating the modulus squared of the permanent of an arbitrary matrix to a smaller additive error, as compared to the additive error estimate obtained from Gurvits algorithm with a run time of $O(t)$. While these results hold for the lossless case only, this leads us to the open question: could recycling mitigation make these claims robust to noise?

Note that there remains the alternative to keep the training phase based on samples only, by using an implicit loss function like the MMD. In our simulations, we tried training a lossless QCBM with the MMD, and obtained similar results. For the lossy case though, this approach would require an extension of the recycling mitigation technique to samples, which would be interesting to investigate.

Other future research directions include explor-

ing mitigation techniques for other types of photonic errors. Also, we noted in our simulations that the initialization of the parameters could significantly affect training. It would be interesting to study this question further, as well as to explore parameter-shift and other optimization methods in the context of photonics. Note that in the longer term, photonic quantum computing is expected to scale through alternative computation models such as measurement-based quantum computing [48]. Several works have begun to explore measurement-based quantum machine learning [49, 50], including QCBMs [51].

CONCLUSION

Our work shows that recycling mitigation can positively impact the training of quantum machine learning models on realistic photonic devices. Given a certain amount of resources, recycling mitigation makes QCBMs that would otherwise be untrainable, for several scenarios. Our work also proposes a straightforward design for a photonic-tailored QCBM, which we hope can be built upon, as we make our code available at <https://github.com/Quandela/photonic-qcbm>.

ACKNOWLEDGEMENTS

The authors would like to thank Eric Bertasi and Marion Fabre for their precious help improving the code, as well as Shane Mansfield and Joseph Bowles for fruitful discussions and feedback on the manuscript. This work has been co-funded by the European Commission as part of the EIC accelerator program under the grant agreement 190188855 for SEPOQC project, by the Horizon-CL4 program under the grant agreement 101135288 for EPIQUE project, and by the OECQ Project financed by the French State as part of France 2030.

* alexia.salavrakos@quandela.com

- [1] D. P. Kingma and M. Welling, in *2nd International Conference on Learning Representations, ICLR 2014, Banff, AB, Canada, April 14-16, 2014, Conference Track Proceedings*, edited by Y. Bengio and Y. LeCun (2014).
- [2] I. Goodfellow, J. Pouget-Abadie, M. Mirza, B. Xu, D. Warde-Farley, S. Ozair, A. Courville, and Y. Bengio, in *Advances in Neural Information Processing Systems*, Vol. 27, edited by Z. Ghahramani, M. Welling, C. Cortes, N. Lawrence, and K. Weinberger (Curran Associates, Inc., 2014).
- [3] J. Sohl-Dickstein, E. Weiss, N. Maheswaranathan, and S. Ganguli, in *Proceedings of the 32nd International Conference on Machine Learning*, Proceedings of Machine Learning Research, Vol. 37, edited by F. Bach and D. Blei (PMLR, Lille, France, 2015) pp. 2256–2265.
- [4] T. Brown, B. Mann, N. Ryder, M. Subbiah, J. D. Kaplan, P. Dhariwal, A. Neelakantan, P. Shyam, G. Sastry, A. Askell, S. Agarwal, A. Herbert-Voss, G. Krueger, T. Henighan, R. Child, A. Ramesh, D. Ziegler, J. Wu, C. Winter, C. Hesse, M. Chen, E. Sigler, M. Litwin, S. Gray, B. Chess, J. Clark, C. Berner, S. McCandlish, A. Radford, I. Sutskever, and D. Amodei, in *Advances in Neural Information Processing Systems*, Vol. 33, edited by H. Larochelle, M. Ranzato, R. Hadsell, M. Balcan, and H. Lin (Curran Associates, Inc., 2020) pp. 1877–1901.
- [5] M. Cerezo, A. Arrasmith, R. Babbush, S. C. Benjamin, S. Endo, K. Fujii, J. R. McClean, K. Mitarai, X. Yuan, L. Cincio, and P. J. Coles, *Nature Reviews Physics* **3**, 625 (2021).
- [6] J. Preskill, *Quantum* **2**, 79 (2018).
- [7] M. Schuld, A. Bocharov, K. M. Svore, and N. Wiebe, *Physical Review A* **101** (2020), [10.1103/physreva.101.032308](https://doi.org/10.1103/physreva.101.032308).
- [8] E. Farhi and H. Neven, arXiv:1802.06002 (2018), [arXiv:1802.06002](https://arxiv.org/abs/1802.06002) [quant-ph].
- [9] J. Tian, X. Sun, Y. Du, S. Zhao, Q. Liu, K. Zhang, W. Yi, W. Huang, C. Wang, X. Wu, M.-H. Hsieh, T. Liu, W. Yang, and D. Tao, arXiv:2206.03066 (2022), [10.48550/ARXIV.2206.03066](https://arxiv.org/abs/2206.03066).
- [10] S. Lloyd and C. Weedbrook, *Physical Review Letters* **121** (2018), [10.1103/physrevlett.121.040502](https://doi.org/10.1103/physrevlett.121.040502).
- [11] P.-L. Dallaire-Demers and N. Killoran, *Physical Review A* **98** (2018), [10.1103/physreva.98.012324](https://doi.org/10.1103/physreva.98.012324).
- [12] A. Khoshaman, W. Vinci, B. Denis, E. Andriyash, H. Sadeghi, and M. H. Amin, *Quantum Science and Technology* **4**, 014001 (2018).
- [13] M. H. Amin, E. Andriyash, J. Rolfe, B. Kulchitskyy, and R. Melko, *Physical Review X* **8** (2018), [10.1103/physrevx.8.021050](https://doi.org/10.1103/physrevx.8.021050).
- [14] N. Wiebe and L. Wossnig, arXiv:1905.09902 (2019), [arXiv:1905.09902](https://arxiv.org/abs/1905.09902) [quant-ph].
- [15] M. Benedetti, D. Garcia-Pintos, O. Perdomo, V. Leyton-Ortega, Y. Nam, and A. Perdomo-Ortiz, *npj Quantum Information* **5** (2019), [10.1038/s41534-019-0157-8](https://doi.org/10.1038/s41534-019-0157-8).
- [16] J.-G. Liu and L. Wang, *Physical Review A* **98** (2018), [10.1103/physreva.98.062324](https://doi.org/10.1103/physreva.98.062324).
- [17] D. Zhu, N. M. Linke, M. Benedetti, K. A. Landsman, N. H. Nguyen, C. H. Alderete, A. Perdomo-Ortiz, N. Korda, A. Garfoot, C. Brecque, L. Egan, O. Perdomo, and C. Monroe, *Science Advances* **5**, eaaw9918 (2019), <https://arxiv.org/abs/1812.08862>.
- [18] M. S. Rudolph, N. B. Toussaint, A. Katabarwa, S. Johri, B. Peropadre, and A. Perdomo-Ortiz,

- Phys. Rev. X **12**, 031010 (2022).
- [19] K. E. Hamilton, E. F. Dumitrescu, and R. C. Pooser, *Phys. Rev. A* **99**, 062323 (2019).
- [20] B. Coyle, M. Henderson, J. C. J. Le, N. Kumar, M. Paini, and E. Kashefi, *Quantum Science and Technology* **6**, 024013 (2021).
- [21] V. Leyton-Ortega, A. Perdomo-Ortiz, and O. Perdomo, *Quantum Mach. Intell.* **3** (2021), [arXiv:1901.08047 \[quant-ph\]](https://arxiv.org/abs/1901.08047).
- [22] N. Maring, A. Fyrillas, M. Pont, E. Ivanov, P. Stepanov, N. Margaria, W. Hease, A. Pishchagin, T. H. Au, S. Boissier, E. Bertasi, A. Baert, M. Valdivia, M. Billard, O. Acar, A. Briussel, R. Mezher, S. C. Wein, A. Salavrakos, P. Sinnott, D. A. Fioretto, P.-E. Emeriau, N. Belabas, S. Mansfield, P. Senellart, J. Senellart, and N. Somaschi, *Nature Photonics* (2024), <https://doi.org/10.1038/s41566-024-01403-4>.
- [23] H.-S. Zhong, H. Wang, Y.-H. Deng, M.-C. Chen, L.-C. Peng, Y.-H. Luo, J. Qin, D. Wu, X. Ding, Y. Hu, P. Hu, X.-Y. Yang, W.-J. Zhang, H. Li, Y. Li, X. Jiang, L. Gan, G. Yang, L. You, Z. Wang, L. Li, N.-L. Liu, C.-Y. Lu, and J.-W. Pan, *Science* **370**, 1460 (2020).
- [24] L. S. Madsen, F. Laudenbach, M. F. Askarani, F. Rortais, T. Vincent, J. F. F. Bulmer, F. M. Miatto, L. Neuhaus, L. G. Helt, M. J. Collins, A. E. Lita, T. Gerrits, S. W. Nam, V. D. Vaidya, M. Menotti, I. Dhand, Z. Vernon, N. Quesada, and J. Lavoie, *Nature* **606**, 75 (2022).
- [25] C. S. Hamilton, R. Kruse, L. Sansoni, S. Barkhofen, C. Silberhorn, and I. Jex, *Physical Review Letters* **119** (2017), [10.1103/physrevlett.119.170501](https://doi.org/10.1103/physrevlett.119.170501).
- [26] D. A. Lidar and T. A. Brun, *Quantum error correction* (Cambridge university press, 2013).
- [27] S. Endo, S. C. Benjamin, and Y. Li, *Physical Review X* **8** (2018), [10.1103/physrevx.8.031027](https://doi.org/10.1103/physrevx.8.031027).
- [28] S. Endo, Z. Cai, S. C. Benjamin, and X. Yuan, *Journal of the Physical Society of Japan* **90**, 032001 (2021).
- [29] J. Mills and R. Mezher, In preparation (2024).
- [30] S. Aaronson and A. Arkhipov, Proceedings of the forty-third annual ACM symposium on Theory of computing , 333 (2011).
- [31] W. R. Clements, P. C. Humphreys, B. J. Metcalf, W. S. Kolthammer, and I. A. Walmsley, *Optica* **3**, 1460 (2016).
- [32] S. Shankar and D. Towsley, in *Joint European Conference on Machine Learning and Knowledge Discovery in Databases. Springer* (2022).
- [33] J. Shi, Y. Tang, Y. Lu, Y. Feng, R. Shi, and S. Zhang, *IEEE Transactions on Knowledge and Data Engineering* **35**, 1965 (2023).
- [34] S. Kullback and R. A. Leibler, *The Annals of Mathematical Statistics* **22**, 79 (1951).
- [35] A. Gretton, K. M. Borgwardt, M. J. Rasch, B. Schölkopf, and A. Smola, *Journal of Machine Learning Research* **13**, 723 (2012).
- [36] M. Schuld, V. Bergholm, C. Gogolin, J. Izaac, and N. Killoran, *Physical Review A* **99** (2019), [10.1103/physreva.99.032331](https://doi.org/10.1103/physreva.99.032331).
- [37] J. G. Vidal and D. O. Theis, “Calculus on parameterized quantum circuits,” (2018), [arXiv:1812.06323 \[quant-ph\]](https://arxiv.org/abs/1812.06323).
- [38] G. de Felice and C. Cortlett, [arXiv:2401.07997](https://arxiv.org/abs/2401.07997) (2024), [arXiv:2401.07997 \[quant-ph\]](https://arxiv.org/abs/2401.07997).
- [39] J. C. Spall, *Johns Hopkins APL Technical Digest* **19**, 482 (1998).
- [40] N. Heurtel, A. Fyrillas, G. de Gliniasty, R. L. Bihan, S. Malherbe, M. Pailhas, E. Bertasi, B. Bourdoncle, P.-E. Emeriau, R. Mezher, L. Music, N. Belabas, B. Valiron, P. Senellart, S. Mansfield, and J. Senellart, *Quantum* **7**, 931 (2023).
- [41] C. Zoufal, [arXiv:2111.12738](https://arxiv.org/abs/2111.12738) (2021), [arXiv:2111.12738 \[quant-ph\]](https://arxiv.org/abs/2111.12738).
- [42] B. Y. Gan, D. Leykam, and D. G. Angelakis, *EPJ Quantum Technology* **9** (2022), [10.1140/epjqt/s40507-022-00135-0](https://doi.org/10.1140/epjqt/s40507-022-00135-0).
- [43] L. Gurvits, in *Mathematical Foundations of Computer Science 2005*, edited by J. Jędrzejowicz and A. Szepietowski (Springer Berlin Heidelberg, Berlin, Heidelberg, 2005) pp. 447–458.
- [44] S. Aaronson and T. Hance, [arXiv:1212.0025](https://arxiv.org/abs/1212.0025) (2012), [arXiv:1212.0025 \[quant-ph\]](https://arxiv.org/abs/1212.0025).
- [45] W. Hoeffding, *The collected works of Wassily Hoeffding* (Springer Science & Business Media, 2012).
- [46] B. Coyle, D. Mills, V. Danos, and E. Kashefi, *npj Quantum Information* **6** (2020), [10.1038/s41534-020-00288-9](https://doi.org/10.1038/s41534-020-00288-9).
- [47] M. S. Rudolph, S. Lerch, S. Thanasilp, O. Kiss, S. Vallecorsa, M. Grossi, and Z. Holmes, [arXiv:2305.02881](https://arxiv.org/abs/2305.02881) (2023), [arXiv:2305.02881 \[quant-ph\]](https://arxiv.org/abs/2305.02881).
- [48] R. Raussendorf and H. J. Briegel, *Phys. Rev. Lett.* **86**, 5188 (2001).
- [49] R. Ferguson, L. Dellantonio, A. A. Balushi, K. Jansen, W. Dür, and C. Muschik, *Physical Review Letters* **126** (2021), [10.1103/physrevlett.126.220501](https://doi.org/10.1103/physrevlett.126.220501).
- [50] H. P. Nautrup and H. J. Briegel, [arXiv:2312.13185](https://arxiv.org/abs/2312.13185) (2023), [arXiv:2312.13185 \[quant-ph\]](https://arxiv.org/abs/2312.13185).
- [51] A. Majumder, M. Krumm, T. Radkohl, H. P. Nautrup, S. Jerbi, and H. J. Briegel, [arXiv:2310.13524](https://arxiv.org/abs/2310.13524) (2023), [arXiv:2310.13524 \[quant-ph\]](https://arxiv.org/abs/2310.13524).
- [52] R. Mezher, A. F. Carvalho, and S. Mansfield, *Physical Review A* **108**, 032405 (2023).

Approximating output probabilities

In this section, we discuss approximating $|\text{Per}(A)|^2$ for an arbitrary $n \times n$ matrix A to a given additive error precision, $\text{Per}(\cdot)$ being the matrix permanent. We show that computing $|\text{Per}(A)|^2$ from statistics collected from t i.i.d runs of a boson sampler produces, with high probability, a more accurate estimate of $|\text{Per}(A)|^2$ than Gurvits which is run for time $O(t)$. More precisely, we show in theorems 1 and 2 that Gurvits algorithm requires a runtime t^* with $t^* = O(n^2 t)$ to produce an additive error approximation of

$|\text{Per}(A)|^2$ of the same order of magnitude as that obtained from $O(t)$ runs of a boson sampler.

Let A be an $n \times n$ matrix with complex entries. Gurvits algorithm [43] provides an estimate $\mathbf{E}(\text{Per}(A))$ of $\text{Per}(A)$, the permanent of A , to within additive precision $\epsilon \|A\|^n$, where $\|A\|$ is the spectral norm of A , and $\epsilon > 0$. More precisely, the output of Gurvits algorithm is $\mathbf{E}(\text{Per}(A))$ such that

$$|\mathbf{E}(\text{Per}(A)) - \text{Per}(A)| \leq \epsilon \|A\|^n.$$

The runtime of Gurvits is $O(\frac{n^2}{\epsilon^2})$, and the above inequality holds with high probability (By Hoeffding's inequality [45]). The $O(n^2)$ part comes from the complexity of computing the Glynn coefficients in Ryser's formula.

We prove the following.

Theorem 1. *For an $n \times n$ matrix A with entries in \mathbb{C} and $\epsilon > 0$, Gurvits algorithm [44] outputs with high probability in $O(\frac{n^2}{\epsilon^2})$ -time an estimate $\mathbf{E}(\text{Per}^2(A))$ such that*

$$||\mathbf{E}(\text{Per}^2(A))| - |\text{Per}^2(A)|| \leq \epsilon(2 + \epsilon) \|A\|^{2n}.$$

Proof. Let $\mathbf{E}(\text{Per}^2(A)) := (\mathbf{E}(\text{Per}(A)))^2$, where $\mathbf{E}(\text{Per}(A))$ is the output of Gurvits algorithm. $|\mathbf{E}(\text{Per}^2(A)) - \text{Per}^2(A)| = |\mathbf{E}(\text{Per}(A)) - \text{Per}(A)| |\mathbf{E}(\text{Per}(A)) + \text{Per}(A)| \leq \epsilon \|A\|^n (|\mathbf{E}(\text{Per}(A))| + |\text{Per}(A)|)$.

Using a reverse triangle inequality

$$\begin{aligned} ||\mathbf{E}(\text{Per}(A))| - |\text{Per}(A)|| &\leq |\mathbf{E}(\text{Per}(A)) - \text{Per}(A)| \\ &\leq \epsilon \|A\|^n, \end{aligned}$$

and consequently $|\mathbf{E}(\text{Per}(A))| \leq |\text{Per}(A)| + \epsilon \|A\|^n$. Plugging this into the inequality of $|\mathbf{E}(\text{Per}^2(A)) - \text{Per}^2(A)|$ gives

$$\begin{aligned} |\mathbf{E}(\text{Per}^2(A)) - \text{Per}^2(A)| &\leq \epsilon \|A\|^n (2|\text{Per}(A)| + \epsilon \|A\|^n) \\ &\leq \epsilon(2 + \epsilon) \|A\|^{2n}, \end{aligned}$$

where the rightmost side follows from $|\text{Per}(A)| \leq \|A\|^n$. To complete the proof, we again use a reverse triangle inequality

$$\begin{aligned} ||\mathbf{E}(\text{Per}^2(A))| - |\text{Per}^2(A)|| &\leq |\mathbf{E}(\text{Per}^2(A)) - \text{Per}^2(A)| \\ &\leq \epsilon(2 + \epsilon) \|A\|^{2n}, \end{aligned}$$

and this completes the proof. \square

Now, we prove an analogue of the above theorem for estimating $|\text{Per}^2(A)|$ from the output statistics of linear optical circuits.

Theorem 2. *Let A be an $n \times n$ matrix with entries in \mathbb{C} , and $\epsilon > 0$. There is a linear optical circuit U which, with $O(\frac{1}{\epsilon^2})$ samples and with high probability outputs an estimate $\mathbf{E}(|\text{Per}^2(A)|)$ such that*

$$|\mathbf{E}(|\text{Per}^2(A)|) - |\text{Per}^2(A)| \leq \epsilon \|A\|^{2n},$$

Proof. Embed A onto a linear optical circuit U using the unitary dilation theorem. From the results of [52], by using Hoeffding's inequality [45], we can with high confidence and with $O(\frac{1}{\epsilon^2})$ samples estimate the probability $p = |\text{Per}^2(A_s)|$ to within precision ϵ , where $A_s := \frac{A}{\|A\|}$. Therefore, we obtain an estimate $\mathbf{E}(|\text{Per}^2(A_s)|)$ as follows

$$|\mathbf{E}(|\text{Per}^2(A_s)|) - |\text{Per}^2(A_s)| \leq \epsilon.$$

Noting that $|\text{Per}^2(A_s)| = \frac{|\text{Per}^2(A)|}{\|A\|^{2n}}$, then multiplying both sides of the above inequality by $\|A\|^{2n}$, and defining $\mathbf{E}(|\text{Per}^2(A)|) := \|A\|^{2n} \mathbf{E}(|\text{Per}^2(A_s)|)$ completes the proof. \square